Rock and Soil Mechanics

Volume 43 | Issue 9 Article 8

10-31-2022

Application of nonlinear soil resistance-pile lateral displacement curve based on Pasternak foundation model in foundation pit retaining piles

Yan-peng ZHU
Western Center of Disaster Mitigation in Civil Engineering of Ministry of Education, Lanzhou University of Technology, Lanzhou, Gansu 730050, China

Lin-ping WU
Western Center of Disaster Mitigation in Civil Engineering of Ministry of Education, Lanzhou University of Technology, Lanzhou, Gansu 730050, China, wlping0916@163.com

Duo-bang SHI
Western Center of Disaster Mitigation in Civil Engineering of Ministry of Education, Lanzhou University of Technology, Lanzhou, Gansu 730050, China

Zhuang-fu ZHAO
Western Center of Disaster Mitigation in Civil Engineering of Ministry of Education, Lanzhou University of Technology, Lanzhou, Gansu 730050, China

See next page for additional authors

Custom Citation

ZHU Yan-peng, WU Lin-ping, SHI Duo-bang, ZHAO Zhuang-fu, LÜ Xiang-xiang, DUAN Xin-guo, . Application of nonlinear soil resistance-pile lateral displacement curve based on Pasternak foundation model in foundation pit retaining piles[J]. Rock and Soil Mechanics, 2022, 43(9): 2581-2591.

Authors

Yan-peng ZHU, Lin-ping WU, Duo-bang SHI, Zhuang-fu ZHAO, Xiang-xiang L, and Xin-guo DUAN

Rock and Soil Mechanics 2022 43(9): 2581–2591
https: //doi.org/10.16285/j.rsm.2021.6936
ISSN 1000–7598
rocksoilmech.researchcommons.org/journal

Application of nonlinear soil resistance-pile lateral displacement curve based on Pasternak foundation model in foundation pit retaining piles

ZHU Yan-peng[1, 2], WU Lin-ping[1, 2], SHI Duo-bang[1, 2], ZHAO Zhuang-fu[1, 2], LÜ Xiang-xiang[1, 2], DUAN Xin-guo[1, 2]

1. Key Laboratory of Disaster Mitigation in Civil Engineering of Gansu Province, Lanzhou University of Technology, Lanzhou, Gansu 730050, China
2. Western Center of Disaster Mitigation in Civil Engineering of Ministry of Education, Lanzhou University of Technology, Lanzhou, Gansu 730050, China

Abstract: As a direct retaining structure in the process of foundation pit excavation, the internal force and deformation of pile under horizontal load have great influence on the safety and economy of foundation pit engineering. In order to calculate the internal force and deformation of the supporting pile more accurately, the nonlinear foundation reaction modulus is obtained according to the nonlinear soil resistance-pile lateral displacement (*p*–*y*) curve of pile-soil interaction. At the same time, the Pasternak two-parameter foundation model is introduced to fully consider the continuity of pile side soil deformation. The differential equation of retaining pile deflection considering pile-anchor deformation coordination is derived, and the internal force and deformation of the retaining pile are obtained by the transfer matrix method. Then the calculation program is compiled based on the engineering example, and the calculation results of the program are compared with the monitoring values and the calculation results of the *p*–*y* curve method based on the traditional Winkler foundation model. It is found that the traditional Winkler foundation model will overestimate the horizontal deformation and internal force of the retaining pile. The displacement and bending moment calculated by the program can better meet the actual requirements of the project. Furthermore, the finite element software is used for numerical simulation analysis of the engineering example to verify the rationality and applicability of the calculation method of foundation pit supporting piles based on the nonlinear Pasternak two-parameter foundation model.

Keywords: foundation pit; retaining pile; *p*–*y* curve; Pasternak two-parameter foundation model; transfer matrix method

1 Introduction

During the design of foundation pit retaining piles, to ensure safety and reduce economic cost, it is necessary to investigate the internal force and deformation of the retaining pile in depth under the action of horizontal loads. At present, the research methods for the stress and deformation analysis of foundation pit retaining piles mainly include on-site monitoring[1], numerical simulation[2], theoretical analysis[3], model tests[4]. In the existing theoretical analysis, the pile side soil is generally regarded as the Winkler foundation model to investigate pile-soil interaction. Based on the Winkle foundation model, Ma et al.[5] investigated the nonlinear dynamic response of laterally loaded long piles by replacing the elastic foundation with independent linear springs. Zhao et al.[6] simplified the horizontal load and soil resistance on the pile side based on the Winkler foundation model, and established a simplified calculation model for laterally loaded piles under the effect of steep slopes. In the above literature, the foundation is regarded as the Winkler elastic foundation, and the soil on the pile side is discretized into independent linear springs, while the continuity of internal force and deformation of soil induced by pile-soil interaction is ignored, which is not consistent with the stress state of piles in actual engineering.

To address the shortcomings of the Winkler foundation model, the two-parameter foundation model takes into account the shear action of the soil around the pile by introducing a second parameter *G*, where *G* is the shear modulus of soil (kN/m). The calculation results are better than those from the conventional single-parameter foundation model. Based on the two-parameter foundation theory, Zhang et al.[7] applied the energy variation principle to the derivation of the deflection differential equation for laterally loaded long piles. The modulus of subgrade reaction was assumed to be constant, and the analytical solution for the lateral displacement of the pile was obtained. Considering the variation of f modulus of subgrade reaction with depth, Liang et al.[8] proposed a simplified analysis method for laterally loaded piles based on the Pasternak two-parameter foundation model. Although the two-parameter foundation model can consider the continuity of lateral soil deformations, it still belongs to the elastic foundation theory. Some researchers believe that the soil resistance increases linearly with the increase of soil deformation. However, in fact, the soil resistance changes nonlinearly with the increase of soil deformation and

Received: 16 November 2021 Revised: 6 May 2022
This work was supported by the General Program of National Natural Science Foundation of China(51978321).
First author: ZHU Yan-peng, male, born in 1960, MSc, Professor, PhD Professor, mainly engaged in teaching and research work in support structure, engineering accident analysis and treatment. E-mail: zhuyp1@163.com
Corresponding author: WU Lin-ping, male, born in 1996, MSc candidate, majoring in support structure. E-mail: wlping0916@163.com

finally tends to a certain critical value.

The *p*–*y* curve can reflect the nonlinear characteristics of pile-soil interaction and is widely used in the analysis of foundation pit retaining piles. Based on the ideal elastic-plastic *p*–*y* curve, Zhu et al.[9] investigated the pile-soil interaction in the deep foundation pit, and derived the pile deflection differential equation considering the pile-anchor deformation coordination. The deformation and internal force of the retaining structure were calculated using the finite difference method. Zhu et al.[10] combined the *p*–*y* curve and unified ultimate resistance to calculate the displacements of foundation retaining piles. The results were compared with those of *m*-method, where *m* is the proportional coefficient of the horizontal resistance coefficient of soil. It is found that when the *p*–*y* curve is applied to the calculation of the foundation pit retaining structure, the calculation results obtained were more consistent with the actual engineering. However, the *p*–*y* curve also has evident shortcomings, that is, the *p*–*y* curves at each position along the pile depth are independent and cannot reflect the mechanical properties of the soil as a continuous medium.

Based on the Pasternak two-parameter foundation model and *p*–*y* curve, a coupled calculation method combining advantages of both methods is proposed in this study. Based on the Pasternak two-parameter foundation model, the continuity of pile side soil deformation is fully considered. Meanwhile, the corresponding soil reaction modulus at different depths of the pile is obtained based on the nonlinear *p*–*y* curve. Then the differential equation for pile deflection is derived considering the pile–anchor deformation coordination. Finally, substituting the obtained soil reaction modulus into the above deflection differential equation, the internal force and deformation of the pile are solved using the transfer matrix method. Therefore, the calculation method of this study not only considers the lateral continuity of the pile side soil deformation through the nonlinear Pasternak two-parameter foundation model, but also reflects the nonlinear characteristics of the pile side soil in different stress states through the obtained soil reaction modulus using the nonlinear *p*–*y* curve. Finally, an engineering example is demonstrated to verify the rationality and applicability of the calculation method in this study.

2 Calculation model development

2.1 Pasternak two-parameter foundation model

Among various two-parameter foundation models, the most reasonable and widely used one is the Pasternak two-parameter foundation model[11]. Based on the Winkler single-parameter foundation model, it assumes that the soil spring is connected to a shear layer that only undergoes shear deformation without compression to consider the mutual shearing effect of the soil along the pile depth. Thus, it reflects the continuity of soil deformation. Compared with the Winkler foundation model, the Pasternak two-parameter foundation model is more theoretically rigorous, and the calculation results are more accurate. It can better reflect the force–deformation characteristics of the soil around the pile.

The shear layer shown in Fig. 1 is the Pasternak two-parameter foundation model. To consider the continuity of soil deformation, it is assumed that there is a medium that produces only shear deformation without compression, which is connected to the Winkler soil springs. For a horizontally loaded pile, the lateral soil perpendicular to the horizontal load plane will generate shear force. Combining the shear force into the soil resistance, the above model can be expressed as

$$p(y,z)=Ky(z)-G\frac{\mathrm{d}^2y}{\mathrm{d}z^2} \tag{1}$$

where $p(y, z)$ is the soil resistance (kN/m); K is the modulus of subgrade reaction (kPa); and z is the depth from the ground surface (m).

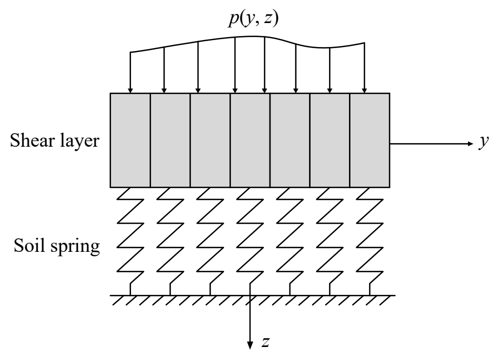

Fig. 1 Pasternak two-parameter foundation model

Therefore, the differential equation for the retaining pile deflection based on the Pasternak two-parameter foundation model can be written as[11]

$$E_pI_p\frac{\mathrm{d}^4y}{\mathrm{d}z^4}-GB\frac{\mathrm{d}^2y}{\mathrm{d}z^2}+KBy=0 \tag{2}$$

where E_p is the elastic modulus of the retaining pile (kPa); I_p is the moment of inertia of the retaining pile cross-section (m^4); and B is the calculation width of the retaining pile cross-section (m).

When the shear modulus G in the above model tends to 0, the Pasternak two-parameter foundation model degenerates into the Winkler foundation model, that is, the Winkler foundation model is an extreme case[12].

In general, the soil shear modulus is closely related to the elastic modulus and Poisson's ratio of the foundation soil, and is obtained according to the solution analogy of the pile–soil interaction problem. Among these solutions, a representative formula for calculating the soil shear modulus is proposed by Tanahashi[13]:

$$G = \frac{E_t t}{6(1+\nu)} \tag{3}$$

where E_t is the elastic modulus of soil (kPa); t is the shear layer thickness of the foundation soil (m); v is the Poisson's ratio of soil.

For the value of the shear layer thickness, according to the numerical simulation results of literature [14], it is considered that the influence zone of the pile side soil is about $11d$ (d is the pile diameter) when subjected to the horizontal load. Therefore, the shear layer thickness can be approximated as $t = 11d$ in this study. In fact, the value of the shear layer thickness is closely related to the properties of the foundation soil. Due to its complexity, the deep investigation is beyond the scope of this study.

When the Pasternak two-parameter foundation model is applied in pile–soil interaction analysis, regardless of the subgrade type, it assumes that the pile and soil are in close contact without gaps during the force and deformation analysis. In addition, the Pasternak two-parameter foundation model can simulate a variety of subgrades ranging from discrete media to continuous media[15].

2.2 *p*–*y* curve

The p–y curve can reflect the real state of soil deformation squeezed by the retaining structure. It connects the resistance p of soil around the pile with the lateral displacement y of the pile under the action of the laterally horizontal thrust. It better reflects the complexity and nonlinearity of pile–soil interaction, which is suitable for the study of foundation pit retaining structures. Many results have been achieved related to the p–y curve model, such as the ideal elastic-plastic model[16], hyperbolic model[17], and various p–y curves fitted using experiments[18].

Kim et al.[19] proposed a hyperbolic p–y model, as shown in Fig. 2. Its form is simple and clear. It conforms to the soil stress–strain relationship, and can better reflects the nonlinear properties of soil. In the initial stage, the modulus of subgrade reaction K_0 is the slope of the tangent line of the curve at the origin. With the increase of the lateral displacement y of the pile, the soil resistance p also increases gradually. The pile undergoes plastic deformation, and the corresponding modulus of subgrade reaction is the secant slope K of the curve ($K = p/y$). When the soil resistance reaches the ultimate soil resistance P_u, the modulus of subgrade reaction tends to 0. Based on the above train of thought, the p–y curve model in this study is chosen as the hyperbolic model, and it can be expressed as

$$p = \frac{y}{\dfrac{1}{K_0} + \dfrac{y}{P_u}} \tag{4}$$

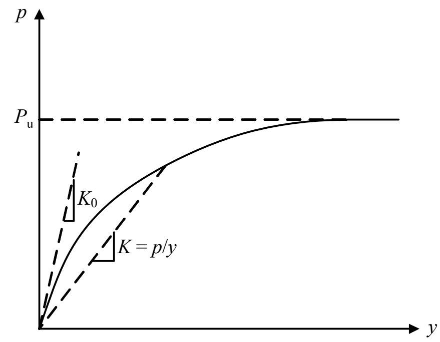

Fig. 2 Hyperbolic *p*–*y* model

2.3 Differential equation for pile deflection

Based on the Pasternak two-parameter foundation model, the continuity of the pile side soil deformation is considered. At the same time, the nonlinear characteristics of soil spring deformation are reflected through the modulus of subgrade reaction calculated using the nonlinear p–y curve. Then the calculation sketch of the pile–anchor retaining structure is established, as shown in Fig. 3, where K_{ti} and K_{tj} are the stiffness coefficients of the i-th and j-th anchor rods, respectively; L_1 and L_2 are the pile lengths above and below the excavation surface, respectively.

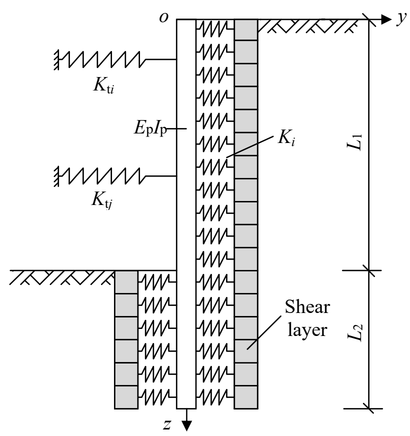

Fig. 3 Calculation diagram of pile–anchor retaining structure in two-parameter foundation model

The soil on both sides of the foundation pit retaining pile is equivalent to soil springs. To consider the force and deformation continuity of the pile side soil, it is assumed that soil springs are connected to a shear layer that produces only shear deformation without compression. Considering the pile–anchor rod deformation coordination, the anchor rod is replaced by a spring and its stiffness coefficient is denoted as K_t.

In this calculation model, the earth pressure is calculated based on the earth pressure at rest, and the tensile force of the anchor rod is based on the initial prestress. It is defined that the active deformation occurs when the displacement y is positive, and the passive deformation occurs when y is negative. Therefore, when the active deformation occurs, the increment of earth pressure is negative and the increment of anchor rod tension is positive; when the passive deformation occurs, the increment of soil resistance is positive and the increment of anchor rod tension is negative[20].

Substituting the above earth pressure and anchor rod tension calculation model into the deflection differential Eq. (2) of the retaining pile of the Pasternak two-parameter foundation model, Eq. (2) for the free section ($0 \leqslant z \leqslant L_1$) can be written as

$$E_{\mathrm{P}} I_{\mathrm{P}} \frac{\mathrm{d}^4 y}{\mathrm{d}z^4} - GB \frac{\mathrm{d}^2 y}{\mathrm{d}z^2} - (P - Ky)B + T_{\mathrm{i}} + K_{\mathrm{t}} y = 0 \qquad (5)$$

where P is the static earth pressure behind the pile in the free section (kN/m); T_{i} is the initial prestress of the anchor rod(kN); and K_{t} is the stiffness coefficient of the elastic fulcrum (kN/m).

Similarly, the deflection differential Eq. (2) for the embedded section ($L_1 \leqslant z \leqslant L_2$) can be written as

$$E_{\mathrm{P}} I_{\mathrm{P}} \frac{\mathrm{d}^4 y}{\mathrm{d}z^4} - 2GB \frac{\mathrm{d}^2 y}{\mathrm{d}z^2} + 2KBy - \Delta PB = 0 \qquad (6)$$

where ΔP is the difference of earth pressure at rest between the two sides of the embedded pile.

3 Determination of calculation parameters

3.1 Initial modulus of subgrade reaction

In the hyperbolic p–y curve model, the initial modulus of subgrade reaction K_0 is usually closely related to the soil elastic modulus. According to the forces of beam with infinite length in three-dimensional elastic half-space, Vesic[21] connected the K_0 with the elastic properties of the pile and soil. However, for horizontally loaded piles, Rajashree et al.[22] conducted a large number of engineering trial calculations and found that the K_0 in the published literature is a little small. They concluded that the initial stiffness K_0 of the p–y curve should be twice the value calculated by the equation proposed by Vesic, which can be expressed by the following equation:

$$K_0 = \frac{1.3E_{\mathrm{t}}}{1 - \nu^2} \left(\frac{E_{\mathrm{t}} B}{E_{\mathrm{p}} I_{\mathrm{p}}} \right) \qquad (7)$$

3.2 Ultimate soil resistance

The determination of the appropriate ultimate soil resistance is crucial to the accuracy of the calculation results for laterally loaded piles. During the construction of the foundation pit retaining structure, due to the change of soil shear strength parameters induced by construction disturbance and retaining structure deformation, the damage modes of soil may be different. As a result, the change of the ultimate soil resistance is difficult to determine. Therefore, it can be solved by using the unified ultimate resistance method[23], and its formula can be expressed as

$$\left.\begin{aligned} &P_{\mathrm{u}} = A_{\mathrm{L}} \left(\alpha_0 + x \right)^n \\ &A_{\mathrm{L}} = N_{\mathrm{p}} \gamma_{\mathrm{s}} d^{2-n} \quad \text{(sand)} \\ &A_{\mathrm{L}} = N_{\mathrm{p}} S_{\mathrm{u}} d^{1-n} \quad \text{(clay)} \end{aligned}\right\} \qquad (8)$$

where A_{L} is the slope of the ultimate soil resistance changing along depth; x is the distance from the calculation point to the ground surface; α_0 is the constant or equivalent soil depth reflecting the magnitude of the ultimate soil resistance on the ground surface; n is the shape parameter of the ultimate resistance; N_{p} is the coefficient of the ultimate resistance; γ_{s} is the effective unit weight of soil; and S_{u} is the undrained shear strength of soil. For sand and clay, A_{L} is calculated using the overburden earth pressure $\gamma_{\mathrm{s}} d$ and undrained shear strength S_{u}, respectively. For sand, $\alpha_0 = 0$, $n = 1.7$, and $N_{\mathrm{p}} = (0.55-1.6) K_{\mathrm{p}}^2$, where K_{p} is the Rankine passive earth pressure coefficient; for clay, $\alpha_0 = 0$–0.5, $n = 0.7$, and $N_{\mathrm{p}} = 0.7$–2.5.

3.3 Coefficient of stiffness for anchor rod

For the determination of K_{t}, the recommended calculation formula by *technical specification for retaining and protection of building foundation excavations* (JGJ 120—2012)[24] is adopted in this study:

$$\left.\begin{aligned} &K_{\mathrm{t}} = \frac{3E_{\mathrm{s}} E_{\mathrm{c}} A_{\mathrm{p}} A b_{\mathrm{a}}}{(3E_{\mathrm{c}} A l_{\mathrm{f}} + E_{\mathrm{s}} A_{\mathrm{p}} l_{\mathrm{a}}) s} \\ &E_{\mathrm{c}} = \frac{E_{\mathrm{s}} A_{\mathrm{p}} + E_{\mathrm{m}} (A - A_{\mathrm{p}})}{A} \end{aligned}\right\} \qquad (9)$$

where E_{s} is the elastic modulus of the anchor rod (kPa); E_{c} is composite elastic modulus of the rod and grouting body (kPa); A_{p} is the cross-sectional area of the anchor rod (m^2); A is the cross-sectional area of the anchorage body (m^2); b_{a} is the calculation width of the of support structure (m); l_{f} is the free length of the anchor rod(m); l_{a} is the anchorage length of the anchor rod(m); s is the horizontal spacing of the anchor (m); and E_{m} is the elastic modulus of the grouting body in the anchorage section (kPa).

4 Internal force and deformation of retaining pile

In this study, the transfer matrix method is used to solve the internal force and deformation of the retaining pile. It is a semi-analytical solution between the finite element solution and the analytical solution[25]. The pile is discretized into sufficient micro-elements according to its characteristics, and the transfer matrix of each micro-element is obtained according to the differential relationship between force and displacement. Then the pile responses can be obtained according to the boundary conditions at both ends of the pile.

For the free section of the pile above the foundation pit excavation surface, it is discretized into N_1 segments. The length of each segment is $h_1 = L_1/N_1$. During the process of discretization, the elastic fulcrum force of the anchor acts on the discrete points. We take micro-element i for analysis, as shown in Fig. 4.

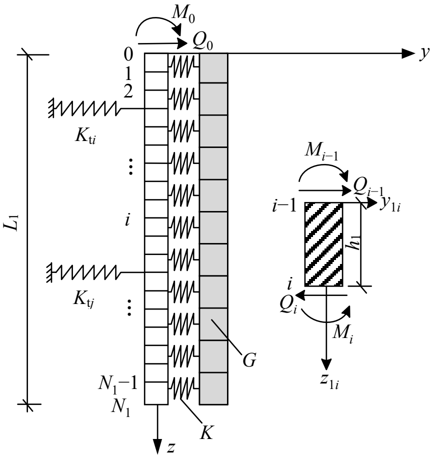

Fig. 4 Calculation diagram of the free section

The governing differential equation for micro-element i can be obtained as

$$E_{\mathrm{p}}I_{\mathrm{p}}\frac{\mathrm{d}^4 y_{1i}}{\mathrm{d}z_{1i}^4}-G_{1i}B\frac{\mathrm{d}^2 y_{1i}}{\mathrm{d}z_{1i}^2}-(P_{1i}-K_{1i}y_{1i})B=0 \tag{10}$$

where y_{1i} is the lateral displacement of the pile of micro-element i in the free section; z_{1i} is the depth calculated from the upper section of micro-element i in the free section; G_{1i} is the soil shear modulus of micro-element i in the free section; P_{1i} is the earth pressure at rest behind the pile of micro-element i in the free section; K_{1i} is the soil reaction modulus of micro-element i in the free section.

By solving the above differential equation, the general solution can be obtained as

$$y_{1i}=C_{1i1}\mathrm{e}^{\alpha_{1i}z_{1i}}\cos(\beta_{1i}z_{1i})+C_{1i2}\mathrm{e}^{\alpha_{1i}z_{1i}}\sin(\beta_{1i}z_{1i})+ C_{1i3}\mathrm{e}^{-\alpha_{1i}z_{1i}}\cos(\beta_{1i}z_{1i})+C_{1i4}\mathrm{e}^{-\alpha_{1i}z_{1i}}\sin(\beta_{1i}z_{1i})+\frac{P_{1i}}{K_{1i}} \tag{11}$$

where C_{1i1}, C_{1i2}, C_{1i3} and C_{1i4} are the coefficients to be determined; and α_{1i} and β_{1i} can be calculated by the following equations:

$$\left.\begin{aligned}\alpha_{1i}&=\sqrt{\sqrt{\frac{K_{1i}B}{4E_{\mathrm{p}}I_{\mathrm{p}}}}+\frac{G_{1i}B}{4E_{\mathrm{p}}I_{\mathrm{p}}}}\\ \beta_{1i}&=\sqrt{\sqrt{\frac{K_{1i}B}{4E_{\mathrm{p}}I_{\mathrm{p}}}}-\frac{G_{1i}B}{4E_{\mathrm{p}}I_{\mathrm{p}}}}\end{aligned}\right\} \tag{12}$$

Then, according to the basic knowledge of material mechanics[26], if the lateral displacement of the upper section of micro-element i is y_{1i}, then its rotation angle θ_{1i}, bending moment M_{1i} and shear force Q_{1i} can be obtained by the following equations:

$$\left.\begin{aligned}\theta_{1i}&=y'_{1i}\\ M_{1i}&=-E_{\mathrm{p}}I_{\mathrm{p}}y''_{1i}\\ Q_{1i}&=-E_{\mathrm{p}}I_{\mathrm{p}}y'''_{1i}\end{aligned}\right\} \tag{13}$$

where

$$\begin{aligned}y'_{1i}=\;&C_{1i1}\left[\alpha_{1i}\mathrm{e}^{\alpha_{1i}z_{1i}}\cos(\beta_{1i}z_{1i})-\beta_{1i}\mathrm{e}^{\alpha_{1i}z_{1i}}\sin(\beta_{1i}z_{1i})\right]+\\ &C_{1i2}\left[\alpha_{1i}\mathrm{e}^{\alpha_{1i}z_{1i}}\sin(\beta_{1i}z_{1i})+\beta_{1i}\mathrm{e}^{\alpha_{1i}z_{1i}}\cos(\beta_{1i}z_{1i})\right]+\\ &C_{1i3}\left[-\alpha_{1i}\mathrm{e}^{-\alpha_{1i}z_{1i}}\cos(\beta_{1i}z_{1i})-\beta_{1i}\mathrm{e}^{-\alpha_{1i}z_{1i}}\sin(\beta_{1i}z_{1i})\right]+\\ &C_{1i4}\left[\beta_{1i}\mathrm{e}^{-\alpha_{1i}z_{1i}}\cos(\beta_{1i}z_{1i})-\alpha_{1i}\mathrm{e}^{-\alpha_{1i}z_{1i}}\sin(\beta_{1i}z_{1i})\right]\end{aligned} \tag{14}$$

$$\begin{aligned}y''_{1i}=\;&C_{1i1}\left[\alpha_{1i}^2\mathrm{e}^{\alpha_{1i}z_{1i}}\cos(\beta_{1i}z_{1i})-\beta_{1i}^2\mathrm{e}^{\alpha_{1i}z_{1i}}\cos(\beta_{1i}z_{1i})-\right.\\ &\left.2\alpha_{1i}\beta_{1i}\mathrm{e}^{\alpha_{1i}z_{1i}}\sin(\beta_{1i}z_{1i})\right]+C_{1i2}\left[\alpha_{1i}^2\mathrm{e}^{\alpha_{1i}z_{1i}}\sin(\beta_{1i}z_{1i})-\right.\\ &\left.\beta_{1i}^2\mathrm{e}^{\alpha_{1i}z_{1i}}\sin(\beta_{1i}z_{1i})+2\alpha_{1i}\beta_{1i}\mathrm{e}^{\alpha_{1i}z_{1i}}\cos(\beta_{1i}z_{1i})\right]+\\ &C_{1i3}\left[\alpha_{1i}^2\mathrm{e}^{-\alpha_{1i}z_{1i}}\cos(\beta_{1i}z_{1i})-\beta_{1i}^2\mathrm{e}^{-\alpha_{1i}z_{1i}}\cos(\beta_{1i}z_{1i})+\right.\\ &\left.2\alpha_{1i}\beta_{1i}e^{-\alpha_{1i}z_{1i}}\sin(\beta_{1i}z_{1i})\right]+C_{1i4}\left[\alpha_{1i}^2\mathrm{e}^{-\alpha_{1i}z_{1i}}\sin(\beta_{1i}z_{1i})-\right.\\ &\left.\beta_{1i}^2\mathrm{e}^{-\alpha_{1i}z_{1i}}\sin(\beta_{1i}z_{1i})-2\alpha_{1i}\beta_{1i}\mathrm{e}^{-\alpha_{1i}z_{1i}}\cos(\beta_{1i}z_{1i})\right]\end{aligned} \tag{15}$$

$$\begin{aligned}y'''_{1i}=\;&C_{1i1}\left[\alpha_{1i}^3\mathrm{e}^{\alpha_{1i}z_{1i}}\cos(\beta_{1i}z_{1i})+\beta_{1i}^3\mathrm{e}^{\alpha_{1i}z_{1i}}\sin(\beta_{1i}z_{1i})-\right.\\ &\left.3\alpha_{1i}^2\beta_{1i}\mathrm{e}^{\alpha_{1i}z_{1i}}\sin(\beta_{1i}z_{1i})-3\alpha_{1i}\beta_{1i}^2\mathrm{e}^{\alpha_{1i}z_{1i}}\cos(\beta_{1i}z_{1i})\right]+\\ &C_{1i2}\left[\alpha_{1i}^3\mathrm{e}^{\alpha_{1i}z_{1i}}\sin(\beta_{1i}z_{1i})-\beta_{1i}^3\mathrm{e}^{\alpha_{1i}z_{1i}}\cos(\beta_{1i}z_{1i})+\right.\\ &\left.3\alpha_{1i}^2\beta_{1i}\mathrm{e}^{\alpha_{1i}z_{1i}}\cos(\beta_{1i}z_{1i})-3\alpha_{1i}\beta_{1i}^2\mathrm{e}^{\alpha_{1i}z_{1i}}\sin(\beta_{1i}z_{1i})\right]+\\ &C_{1i3}\left[-\alpha_{1i}^3\mathrm{e}^{-\alpha_{1i}z_{1i}}\cos(\beta_{1i}z_{1i})+\beta_{1i}^3\mathrm{e}^{-\alpha_{1i}z_{1i}}\sin(\beta_{1i}z_{1i})-\right.\\ &\left.3\alpha_{1i}^2\beta_{1i}\mathrm{e}^{-\alpha_{1i}z_{1i}}\sin(\beta_{1i}z_{1i})+3\alpha_{1i}\beta_{1i}^2\mathrm{e}^{-\alpha_{1i}z_{1i}}\cos(\beta_{1i}z_{1i})\right]+\\ &C_{1i4}\left[-\alpha_{1i}^3\mathrm{e}^{-\alpha_{1i}z_{1i}}\sin(\beta_{1i}z_{1i})-\beta_{1i}^3\mathrm{e}^{-\alpha_{1i}z_{1i}}\cos(\beta_{1i}z_{1i})-\right.\\ &\left.3\alpha_{1i}^2\beta_{1i}e^{-\alpha_{1i}z_{1i}}\cos(\beta_{1i}z_{1i})+3\alpha_{1i}\beta_{1i}^2e^{-\alpha_{1i}z_{1i}}\sin(\beta_{1i}z_{1i})\right]\end{aligned} \tag{16}$$

Combining Eqs. (11)–(16), the relationships among the horizontal displacement, cross-section rotation angle, bending moment and shear force of micro-element i of the retaining pile in the free section and the coefficients to be determined can be obtained:

$$[y_{1i},\theta_{1i},M_{1i},Q_{1i},1]^{\mathrm{T}}=[A_{1i}][C_{1i1},C_{1i2},C_{1i3},C_{1i4},1]^{\mathrm{T}} \tag{17}$$

where

$$[A_{1i}]=[\boldsymbol{A}_1,\ \boldsymbol{A}_2,\ \boldsymbol{A}_3,\ \boldsymbol{A}_4,\ \boldsymbol{A}_5]^{\mathrm{T}}$$

$$\boldsymbol{A}_1=\begin{bmatrix} \mathrm{e}^{\alpha_{1i}z_{1i}}\cos(\beta_{1i}z_{1i}) \\ \mathrm{e}^{\alpha_{1i}z_{1i}}\sin(\beta_{1i}z_{1i}) \\ \mathrm{e}^{-\alpha_{1i}z_{1i}}\cos(\beta_{1i}z_{1i}) \\ \mathrm{e}^{-\alpha_{1i}z_{1i}}\sin(\beta_{1i}z_{1i}) \\ P_{1i}/K_{1i} \end{bmatrix}^{\mathrm{T}} \tag{18}$$

$$\boldsymbol{A}_2=\begin{bmatrix} \alpha_{1i}\mathrm{e}^{\alpha_{1i}z_{1i}}\cos(\beta_{1i}z_{1i})-\beta_{1i}\mathrm{e}^{\alpha_{1i}z_{1i}}\sin(\beta_{1i}z_{1i}) \\ \alpha_{1i}\mathrm{e}^{\alpha_{1i}z_{1i}}\sin(\beta_{1i}z_{1i})+\beta_{1i}\mathrm{e}^{\alpha_{1i}z_{1i}}\cos(\beta_{1i}z_{1i}) \\ -\alpha_{1i}\mathrm{e}^{-\alpha_{1i}z_{1i}}\cos(\beta_{1i}z_{1i})-\beta_{1i}\mathrm{e}^{-\alpha_{1i}z_{1i}}\sin(\beta_{1i}z_{1i}) \\ \beta_{1i}\mathrm{e}^{-\alpha_{1i}z_{1i}}\cos(\beta_{1i}z_{1i})-\alpha_{1i}\mathrm{e}^{-\alpha_{1i}z_{1i}}\sin(\beta_{1i}z_{1i}) \\ 0 \end{bmatrix}^{\mathrm{T}} \tag{19}$$

$$\boldsymbol{A}_3=\begin{bmatrix} -E_\mathrm{p}I_\mathrm{p}[\alpha_{1i}^2\mathrm{e}^{\alpha_{1i}z_{1i}}\cos(\beta_{1i}z_{1i})-\beta_{1i}^2\mathrm{e}^{\alpha_{1i}z_{1i}}\cos(\beta_{1i}z_{1i})-2\alpha_{1i}\beta_{1i}\mathrm{e}^{\alpha_{1i}z_{1i}}\sin(\beta_{1i}z_{1i})] \\ -E_\mathrm{p}I_\mathrm{p}[\alpha_{1i}^2\mathrm{e}^{\alpha_{1i}z_{1i}}\sin(\beta_{1i}z_{1i})-\beta_{1i}^2\mathrm{e}^{\alpha_{1i}z_{1i}}\sin(\beta_{1i}z_{1i})+2\alpha_{1i}\beta_{1i}\mathrm{e}^{\alpha_{1i}z_{1i}}\cos(\beta_{1i}z_{1i})] \\ -E_\mathrm{p}I_\mathrm{p}[\alpha_{1i}^2\mathrm{e}^{-\alpha_{1i}z_{1i}}\cos(\beta_{1i}z_{1i})-\beta_{1i}^2\mathrm{e}^{-\alpha_{1i}z_{1i}}\cos(\beta_{1i}z_{1i})+2\alpha_{1i}\beta_{1i}\mathrm{e}^{-\alpha_{1i}z_{1i}}\sin(\beta_{1i}z_{1i})] \\ -E_\mathrm{p}I_\mathrm{p}[\alpha_{1i}^2\mathrm{e}^{-\alpha_{1i}z_{1i}}\sin(\beta_{1i}z_{1i})-\beta_{1i}^2\mathrm{e}^{-\alpha_{1i}z_{1i}}\sin(\beta_{1i}z_{1i})-2\alpha_{1i}\beta_{1i}\mathrm{e}^{-\alpha_{1i}z_{1i}}\cos(\beta_{1i}z_{1i})] \\ 0 \end{bmatrix}^{\mathrm{T}} \tag{20}$$

$$\boldsymbol{A}_4=\begin{bmatrix} -E_\mathrm{p}I_\mathrm{p}[\alpha_{1i}^3\mathrm{e}^{\alpha_{1i}z_{1i}}\cos(\beta_{1i}z_{1i})+\beta_{1i}^3\mathrm{e}^{\alpha_{1i}z_{1i}}\sin(\beta_{1i}z_{1i})-3\alpha_{1i}^2\beta_{1i}\mathrm{e}^{\alpha_{1i}z_{1i}}\sin(\beta_{1i}z_{1i})-3\alpha_{1i}\beta_{1i}^2\mathrm{e}^{\alpha_{1i}z_{1i}}\cos(\beta_{1i}z_{1i})] \\ -E_\mathrm{p}I_\mathrm{p}[\alpha_{1i}^3\mathrm{e}^{\alpha_{1i}z_{1i}}\sin(\beta_{1i}z_{1i})-\beta_{1i}^3\mathrm{e}^{\alpha_{1i}z_{1i}}\cos(\beta_{1i}z_{1i})+3\alpha_{1i}^2\beta_{1i}\mathrm{e}^{\alpha_{1i}z_{1i}}\cos(\beta_{1i}z_{1i})-3\alpha_{1i}\beta_{1i}^2\mathrm{e}^{\alpha_{1i}z_{1i}}\sin(\beta_{1i}z_{1i})] \\ -E_\mathrm{p}I_\mathrm{p}[-\alpha_{1i}^3\mathrm{e}^{-\alpha_{1i}z_{1i}}\cos(\beta_{1i}z_{1i})+\beta_{1i}^3\mathrm{e}^{-\alpha_{1i}z_{1i}}\sin\cos(\beta_{1i}z_{1i})-3\alpha_{1i}^2\beta_{1i}\mathrm{e}^{-\alpha_{1i}z_{1i}}\sin(\beta_{1i}z_{1i})+3\alpha_{1i}\beta_{1i}^2\mathrm{e}^{-\alpha_{1i}z_{1i}}\cos(\beta_{1i}z_{1i})] \\ -E_\mathrm{p}I_\mathrm{p}[-\alpha_{1i}^3\mathrm{e}^{-\alpha_{1i}z_{1i}}\sin(\beta_{1i}z_{1i})-\beta_{1i}^3\mathrm{e}^{-\alpha_{1i}z_{1i}}\cos(\beta_{1i}z_{1i})-3\alpha_{1i}^2\beta_{1i}\mathrm{e}^{-\alpha_{1i}z_{1i}}\cos(\beta_{1i}z_{1i})+3\alpha_{1i}\beta_{1i}^2\mathrm{e}^{-\alpha_{1i}z_{1i}}\sin(\beta_{1i}z_{1i})] \\ 0 \end{bmatrix}^{\mathrm{T}} \tag{21}$$

$$\boldsymbol{A}_5=[0\ \ 0\ \ 0\ \ 0\ \ 1]^{\mathrm{T}} \tag{22}$$

Assuming that the state vector of the upper section of micro-element i is $\boldsymbol{W}_{1i}^{\mathrm{u}}=[y_{1i}(0)\ \theta_{1i}(0)\ M_{1i}(0)\ Q_{1i}(0)\ 1]^{\mathrm{T}}$, and the state vector of the lower section is $\boldsymbol{W}_{1i}^{\mathrm{d}}=[y_{1i}(h_i)\ \theta_{1i}(h_i)\ M_{1i}(h_i)\ Q_{1i}(h_i)\ 1]^{\mathrm{T}}$. Then, based on Eq. (17), the coefficient matrix can be obtained as

$$\begin{bmatrix} C_{1i1} \\ C_{1i2} \\ C_{1i3} \\ C_{1i3} \\ 1 \end{bmatrix}=\left[A_{1i}\right]_{z_{1i}=0}^{-1}\begin{bmatrix} y_{1i}(0) \\ \theta_{1i}(0) \\ M_{1i}(0) \\ Q_{1i}(0) \\ 1 \end{bmatrix} \tag{23}$$

Substituting Eq. (23) into Eq. (17), the state vector transfer relationship between the upper and lower sections of micro-element i is obtained as

$$\begin{bmatrix} y_{1i}(h_1) \\ \theta_{1i}(h_1) \\ M_{1i}(h_1) \\ Q_{1i}(h_1) \\ 1 \end{bmatrix}=\left[A_{1i}\right]_{z_{1i}=h_1}\left[A_{1i}\right]_{z_{1i}=0}^{-1}\begin{bmatrix} y_{1i}(0) \\ \theta_{1i}(0) \\ M_{1i}(0) \\ Q_{1i}(0) \\ 1 \end{bmatrix} \tag{24}$$

Let $\boldsymbol{U}_{1i}=[A_{1i}]_{z_{1i}=h_1}[A_{1i}]_{z_{1i}=0}^{-1}$, then Eq. (24) can be simplified as

$$\boldsymbol{W}_{1i}^{\mathrm{d}}=\boldsymbol{U}_{1i}\cdot\ \boldsymbol{W}_{1i}^{\mathrm{u}} \tag{25}$$

where $\boldsymbol{U}_{1i}$ is the transfer matrix of micro-element i.

According to the continuity of the force and deformation of the retaining pile, the state vector of the upper section of micro-element i happens to be the state vector of the lower section of micro-element $i-1$. Therefore, the following equation can be obtained:

$$\boldsymbol{W}_{1i}^{\mathrm{d}}=\boldsymbol{U}_{1i}\cdot\ \boldsymbol{W}_{1(i-1)}^{\mathrm{d}} \tag{26}$$

Assuming that the prestressed anchor acts on the node j of the pile and the prestress is $T_{(j)}$, then the internal force and displacement at this point will change abruptly. In the transfer matrix method, the point matrix is introduced to consider the effect of the prestressed anchor on the pile. Considering the pile−anchor deformation coordination, the anchor rod is simplified as a spring with a stiffness coefficient of K_t in the calculation model of this study. Therefore, the sudden change $Q'_{1(j)}$ of shear force of the prestressed anchor rod at node j is

$$Q'_{1(j)}=Q_{1(j)}+\left(K_{t(j)}y_{1(j)}+T_{(j)}\right) \tag{27}$$

where $Q_{1(j)}$ is the mutation matrix caused by the concentrated force; $K_{t(j)}$ is the stiffness coefficient of the j-th anchor rod; $y_{1(j)}$ is the corresponding pile shaft deflection at the j-th anchor rod.

Therefore, the transfer matrix at node j can be expressed as

$$\boldsymbol{W}_{1(j)}^{\mathrm{d}}=\boldsymbol{U}_{1(j)}\cdot\ \boldsymbol{W}_{1(j)}^{\mathrm{u}} \tag{28}$$

where $\boldsymbol{W}_{1(j)}^{\mathrm{u}}$ and $\boldsymbol{W}_{1(j)}^{\mathrm{d}}$ are the state vectors of the upper and lower sections at action node j of the prestressed anchor rod, respectively; and $\boldsymbol{U}_{1(j)}$ is the point matrix at the action node of the prestressed anchor rod, and

$$\boldsymbol{U}_{1(j)}=\begin{bmatrix} 1 & 0 & 0 & 0 & 0 \\ 0 & 1 & 0 & 0 & 0 \\ 0 & 0 & 1 & 0 & 0 \\ K_{t(j)} & 0 & 0 & 1 & T_{(j)} \\ 0 & 0 & 0 & 0 & 1 \end{bmatrix} \tag{29}$$

Therefore, the matrix transfer relationship of the retaining pile in the entire free section is

$$\boldsymbol{W}_{1N_1}^{\mathrm{d}}=\boldsymbol{U}_1\cdot\ \boldsymbol{W}_{11}^{\mathrm{u}} \tag{30}$$

where $\boldsymbol{U}_1=\boldsymbol{U}_{1N_1}\boldsymbol{U}_{1(N_1-1)}\cdots\boldsymbol{U}_{1(j)}\cdots\boldsymbol{U}_{12}\boldsymbol{U}_{11}$ is the total transfer matrix of the retaining pile in the free section; $\boldsymbol{U}_{1N_1}$ is the transfer matrix of micro-element N_1 in the free section; $\boldsymbol{W}_{11}^{\mathrm{u}}$ and $\boldsymbol{W}_{1N_1}^{\mathrm{d}}$ are the state vectors of the pile top and the junction between the free section and embedded section, respectively.

4.2 Solution of governing differential equation in embedded section

Similarly, the embedded section of the retaining pile is discretized into N_2 segments. The length of each segment is $h_2 = L_2/N_2$. We take micro-element i for analysis, as shown in Fig. 5.

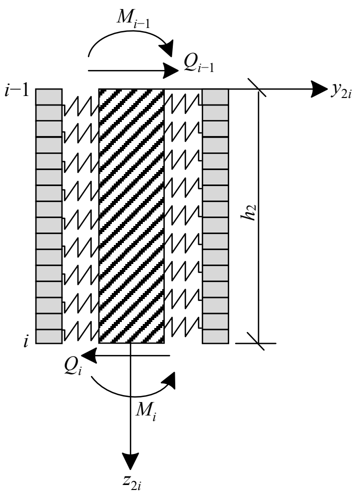

Fig. 5 Calculation diagram of the embedded section

The governing differential equation of micro-element i can be obtained as

$$E_{\mathrm{P}}I_{\mathrm{P}}\frac{\mathrm{d}^4 y_{2i}}{\mathrm{d}z_{2i}^4} - 2G_{2i}B\frac{\mathrm{d}^2 y_{2i}}{\mathrm{d}z_{2i}^2} + 2K_{2i}By_{2i} - \Delta P_{2i}B = 0 \quad (31)$$

where y_{2i} is the lateral displacement of micro-element i in the embedded section; z_{2i} is the depth calculated from the upper section of micro-element i in the embedded section; G_{2i} is the soil shear modulus of micro-element i in the embedded section; ΔP_{2i} is the difference of earth pressure at rest on both pile sides of micro-element i in the embedded section; K_{2i} is the soil reaction modulus of micro-element i in the embedded section.

The general solution form of the governing differential equation of micro-element i in the embedded section is the same as that of the governing differential equation of micro-element i in the free section. The state vector transfer relationship of micro-element i can be obtained by the same derivation method as that of the free section retaining pile:

$$\boldsymbol{W}_{2i}^{\mathrm{d}} = \boldsymbol{U}_{2i} \cdot \boldsymbol{W}_{2i}^{\mathrm{u}} \quad (32)$$

where $\boldsymbol{W}_{2i}^{\mathrm{u}} = [y_{2i}(0)\ \ \theta_{2i}(0)\ \ M_{2i}(0)\ \ Q_{2i}(0)\ \ 1]^{\mathrm{T}}$ is the state vector of the upper section of micro-element i; $\boldsymbol{U}_{2i}$ is the transfer matrix of micro-element i; $\boldsymbol{W}_{2i}^{\mathrm{d}} = [y_{2i}(h_i)\ \ \theta_{2i}(h_i)\ \ M_{2i}(h_i)\ \ Q_{2i}(h_i)\ \ 1]^{\mathrm{T}}$ is the state vector of the lower section of micro-element i.

Similarly, according to the continuity of the force and deformation of the retaining pile in the embedded section, the matrix transfer relationship of the retaining pile in the entire embedded section can be obtained as

$$\boldsymbol{W}_{2N_2}^{\mathrm{d}} = \boldsymbol{U}_2 \cdot \boldsymbol{W}_{21}^{\mathrm{u}} \quad (33)$$

where $\boldsymbol{W}_{2N_2}^{\mathrm{d}}$ and $\boldsymbol{W}_{21}^{\mathrm{u}}$ are the state vectors of the pile bottom and the junction between the embedded section and free section, respectively; $\boldsymbol{U}_2 = \boldsymbol{U}_{2N_2}\boldsymbol{U}_{2(N_2-1)}\cdots\boldsymbol{U}_{2i}\cdots\boldsymbol{U}_{22}\boldsymbol{U}_{21}$ is the total transfer matrix of the retaining pile in the embedded section; $\boldsymbol{U}_{2N_2}$ is the transfer matrix of micro-element N_2 in the embedded section.

For the entire retaining pile, the embedded section and the free section are connected through the continuity condition ($\boldsymbol{W}_{21}^{\mathrm{u}} = \boldsymbol{W}_{1N_1}^{\mathrm{d}}$). Then combining Eqs. (30) and (33), the state vector transfer relationship of the entire retaining pile can be obtained:

$$\boldsymbol{W}_{2N_2}^{\mathrm{d}} = \boldsymbol{U}_2\boldsymbol{U}_1 \cdot \boldsymbol{W}_{11}^{\mathrm{u}} \quad (34)$$

4.3 Boundary conditions

The boundary conditions at both ends of the retaining pile are

$$\left.\begin{array}{ll} M_{11}^{\mathrm{u}} = M_0,\ V_{11}^{\mathrm{u}} = V_0 & \text{(pile top free)} \\ y_{11}^{\mathrm{u}} = 0,\ \theta_{11}^{\mathrm{u}} = 0 & \text{(pile top fixed)} \end{array}\right\} \quad (35)$$

$$\left.\begin{array}{ll} M_{2N_2}^{\mathrm{d}} = 0,\ V_{2N_2}^{\mathrm{d}} = 0 & \text{(pile bottom free)} \\ y_{2N_2}^{\mathrm{d}} = 0,\ \theta_{1N_2}^{\mathrm{d}} = 0 & \text{(pile bottom fixed)} \end{array}\right\} \quad (36)$$

where M_{11}^{u} and M_0 are the bending moment parameters of the retaining pile top boundary and known bending moment, respectively; V_{11}^{u} and V_0 are the shear force parameters of the retaining pile top boundary and known shear force, respectively; θ_{11}^{u} is the rotation angle parameter of the cross section of the retaining pile top boundary; $M_{2N_2}^{\mathrm{d}}$ is the bending moment parameter of the retaining pile bottom boundary; $V_{2N_2}^{\mathrm{d}}$ is the shear force parameter of the retaining pile bottom boundary; $\theta_{1N_2}^{\mathrm{d}}$ is the rotation angle parameter of the cross section of the retaining pile bottom boundary; y_{11}^{u} is the lateral displacement parameter of the retaining pile top boundary; $y_{2N_2}^{\mathrm{d}}$ is the lateral displacement parameter of the retaining pile bottom boundary.

Substituting the boundary conditions into Eq. (34), the state vector $\boldsymbol{W}_{11}^{\mathrm{u}}$ of the pile top can be obtained. Through the recurrence Eq. (37) from Eqs. (26) and (32), the state response of any section can be solved.

$$\left.\begin{array}{l} \boldsymbol{W}_{1i}^{\mathrm{d}} = \boldsymbol{U}_{1i}\boldsymbol{U}_{1(i-1)}\cdots\boldsymbol{U}_{11} \cdot \boldsymbol{W}_{11}^{\mathrm{u}} \\ \boldsymbol{W}_{2i}^{\mathrm{d}} = \boldsymbol{U}_{2i}\boldsymbol{U}_{2(i-1)}\cdots\boldsymbol{U}_{21} \cdot \boldsymbol{W}_{21}^{\mathrm{u}} \end{array}\right\} \quad (37)$$

In the initial calculation stage, the modulus of subgrade reaction substituted into the calculation matrix is the initial value obtained from the hyperbolic p–y curve. As a result, the obtained pile displacement is not accurate. Therefore, it is necessary to obtain more accurate internal force and deformation values of the pile by iteration. The specific calculation process is shown in Fig. 6.

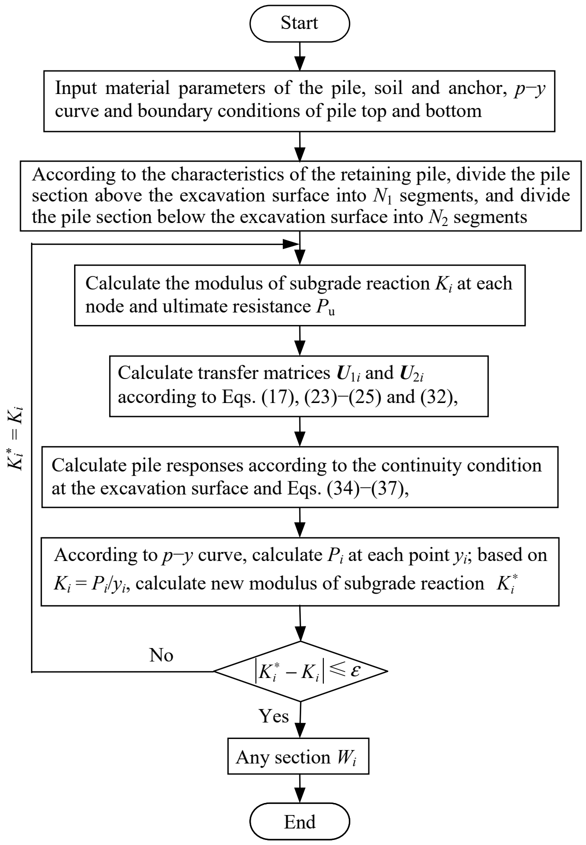

Fig. 6 Flow chart of calculation

5 Model verification and example analysis

5.1 Accuracy and rationality

To verify the rationality of the shear layer assumption in the Pasternak two-parameter foundation model, based on the calculation example in literature [27], the results of this study are compared with those of the literatures. The horizontally loaded isolated pile had a length of 4.65 m, a diameter of 0.36 m and an elastic modulus of 20 GPa. The elastic modulus of foundation soil was 9 233 kPa, and the Poisson’s ratio was 0.3. The pile top was free. The pile was subjected to a horizontal load of 60 kN and a bending moment of 69 kN·m. According to the solving method of the governing differential equation of the embedded section, the lateral displacement of the horizontal isolated pile is calculated. The pile is discretized into 53 segments with each section being 0.05 m long, and the calculation program is compiled according to the calculation flow of Fig. 6. The calculation results are shown in Fig. 7.

As shown in Fig. 7, the variation pattern of the pile lateral displacement in this study is in consistent with that in the literature, and the maximum value of the pile lateral displacement occurs at the top position of the pile. In addition, the calculated results of this paper are in good agreement with those of the finite element method and the experiment. It indicates that the Pasternak two-parameter foundation model can better reflect the pile deformation pattern when applied to the calculation of horizontally loaded piles, which proves the rationality of the shear layer assumption.

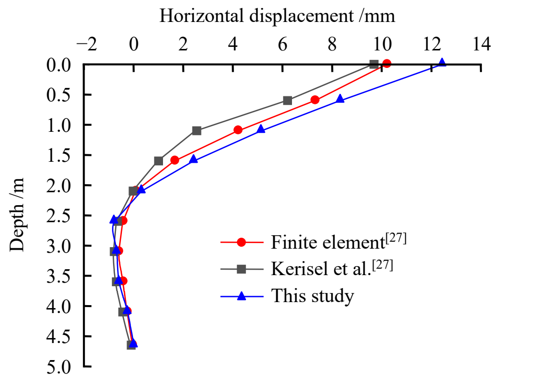

Fig. 7 Comparison curves of horizontal displacements of piles

5.2 Project profile

We take the deep foundation pit of the Lanzhou Zhonghai Plaza construction project in literature [28] as an example. The surrounding environment of this pit is complex, and the pile-anchor structure retaining section on the east side of the foundation pit is selected for calculation and analysis. The depth of the foundation pit is 12.7 m. The retaining pile has a length of 19.0 m, a diameter of 0.8 m, and a spacing of 2.0 m. The embedded pile depth is 6.3 m. The compressive stiffness and bending stiffness of the pile are 6.03×10^7 kN and 9.4×10^5 kN·m^2, respectively. The prestressed anchor cables are installed at 3 m and 6 m from the pit top, respectively. The length of the free section is 6.0 m, and the length of the anchorage section is 10.0 m. The anchor cable is composed of three bundles of ϕ_s15.2 mm steel strands with an inclination angle of 15º, tensile strength of 1 860 MPa, elastic modulus of 1.95×105 MPa, and cross-sectional area of 140 mm^2 for each bundle, respectively. A pretension stress of 160 kN is applied to the anchor cable. M20 grade cement grout is adopted for grouting. The diameter of anchorage body is 150 mm. Other parameters are shown in Fig. 8. The safety factor of the foundation pit is Level 1. The soil parameters provided by the geotechnical engineering survey and test report are shown in Table 1.

5.3 Calculation and analysis

The general finite element software Plaxis 2D in geotechnical engineering is used for numerical simulation analysis of the excavation process of the pile-anchor retaining foundation pit in the engineering example. The finite element calculation model is established, as shown in Fig. 9. The model dimension is 60 m in width and

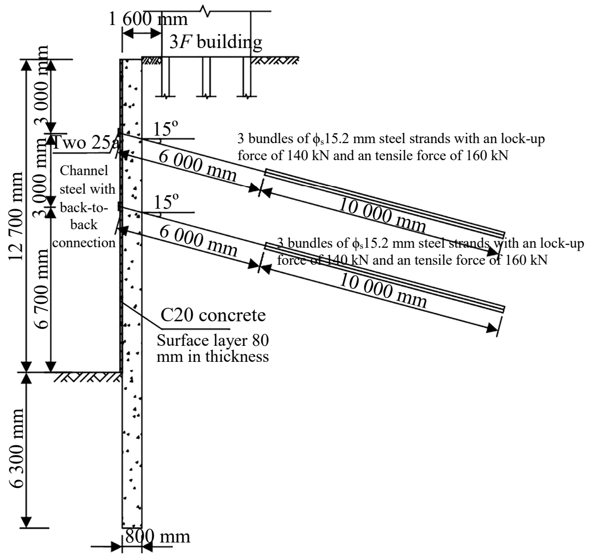

Fig. 8 Section of pile-anchor structure retaining scheme

Table 1 Physical and mechanical indexes of the soil layer

Soil layer	Thickness /m	Unit weight γ/(kN • m^{-3})	Cohesion c /kPa	Friction angle φ/(°)	Friction with anchor rod /kPa
Miscellaneous soil	2.1	17.0	8.0	15.0	30
Silty fine sand	4.7	18.0	10.0	25.0	40
Loess-like silt	5.9	17.0	20.0	26.0	70
Fine sand	1.1	18.0	0.0	30.0	70
Pebble	4.3	23.0	0.0	45.0	220

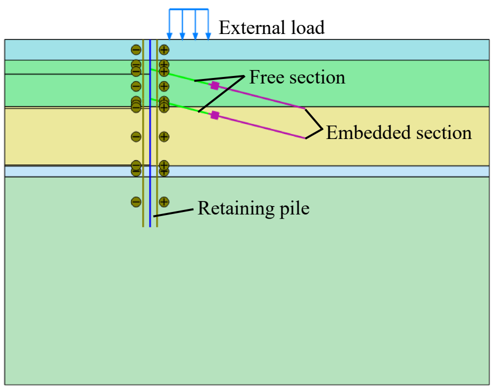

Fig. 9 Finite element calculation model

40 m in height. The Mohr-Coulomb ideal elastic-plastic model is used to simulate soil materials. The free section of the pretressed anchor is simulated by point-to-point anchor rod elements, and the anchorage section is simulated by geogrid elements. The retaining pile is simulated by plate elements. The boundary conditions are taken as follows: the horizontal displacements on both sides is 0, and the displacement on the bottom side is 0. The main construction conditions of the foundation excavation are shown in Table 2.

From Fig. 10, it can be observed that the maximum lateral displacement of the pile occurs at about 5/7 times the pit depth after excavation. One set of anchor cables are installed separately at 3.0 m and 6.0 m away from the pit top, and a prestress of 160 kN is applied. In contrast, there are no anchor cables between 6.0 m and 12.7 m from the pit top. As a result, the earth pressure behind the pile is balanced by the pile itself, which leads to the appearance of the maximum lateral displacement of 17.56 mm at a depth of about 9 m (see Fig. 11). However, the lateral displacement of the pile satisfies the requirement of the specification[29]. The entire foundation pit is in a safe state during the excavation process.

Table 2 Main construction conditions

Condition	Excavation depth /m	Explanation
1	3.5	Set up the first set of anchor cable at depth of 3.0 m
2	6.5	Set up the first set of anchor cable at depth of 6.5 m
3	12.7	Excavate to the pit bottom

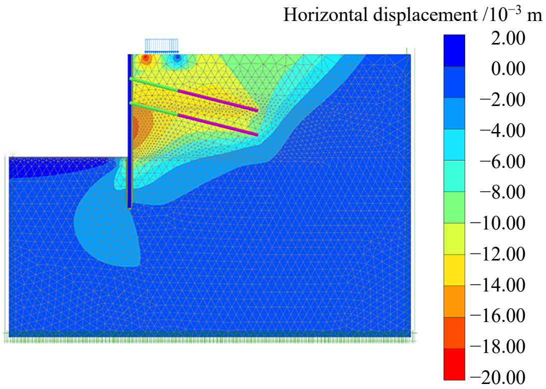

Fig. 10 Nephogram of overall horizontal displacements after excavation

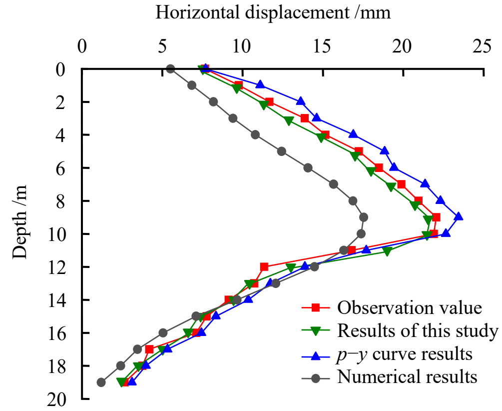

Fig. 11 Comparison curves of horizontal displacements of piles

According to the analysis of laterally loaded piles in literature [22], the mechanical properties of laterally loaded piles mainly depend on the ultimate resistance of the shallow soils. Therefore, in this study, take n = 0.7, α_0 = 0.35 and N_p = 2.2. Substituting the calculation parameters in the engineering example into the compiled calculation program, the lateral displacements and bending moments of the retaining pile based on the nonlinear Pasternak two-parameter foundation model (hereinafter referred to as the solution of this study) and those based on the p–y curve method of the Winkler foundation model (hereinafter referred to as the solution of the *p*–*y* curve method) are obtained.

It can be seen from Fig. 11 that: (1) The variation trends of the pile side displacement curves calculated by the method in this study, the traditional *p*–*y* curve method and the finite element method are basically the same, and the location of the maximum lateral displacement of the pile also tends to be the same, all appearing at the depth of about 9 m. (2) The calculation results of the method in this study and the traditional *p*–*y* curve method are obviously closer to the measured values than that by the finite element, indicating that the finite element software is more conservative when calculating the retaining piles. (3) Compared with the finite element method and the traditional *p*–*y* curve method, both the variation pattern and the maximum value of the pile lateral displacement in this study are closer to the measured values. Especially above the excavation surface of the foundation pit, this phenomenon is more obvious. It indicates that the calculation accuracy is significantly improved when the shearing effect of the soil is considered. (4) The solution of this study is generally smaller than that of the *p*–*y* curve method. The maximum pile lateral displacements of the solution of this study, *p*–*y* curve method, and finite element method are 21.32, 23.58 and 21.56 mm, respectively. The deviations of the former two results from the measured results are 1.1% and 10.0%, respectively. This is due to the fact that the solution of the *p*–*y* curve method is obtained based on the Winkler foundation model. It does not consider the continuity of the soil deformation, which leads to the larger calculation results. It indicates that the shear effect of the soil on the pile side contributes to the reduction of the pile lateral displacement in a certain degree. (5) As the foundation pit excavation continues, the pile lateral displacements all begin to decrease after reaching the maximum values. The pile lateral displacements by this study, the *p*–*y* curve method and the measured values are gradually close to the numerical results. This indicates that with the increase of excavation depth, the lateral displacements at different pile depths will increase cumulatively, and the soil resistance will gradually decrease, so that the earth pressure difference acting on the retaining pile gradually decreases.

Figure 12 illustrates that the maximum negative bending moments of the pile estimated by this study, the *p*–*y* curve method and numerical simulation are −470.35, −532.14 and −440.53 kN·m, respectively. The maximum negative bending moments appear at the pile depth of about 10 m. The maximum positive bending moments of the pile obtained from this study, the *p*–*y* curve method and numerical simulation are 250.69, 280.73 and 224.56 kN·m, respectively. The maximum positive bending moments appear at the pile depth of about 15 m. However, the differences in the trends of the pile moment curves obtained by the three methods are not significant. The maximum positive and negative bending moments obtained by the *p*–*y* curve method increase by 12.04% and 13.20%, respectively, compared with those of this study. This indicates that the Winkler foundation beam model slightly overestimates the distribution of bending moments.

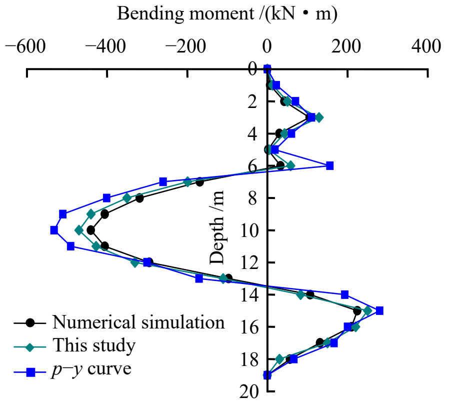

Fig. 12 Comparison curves of pile bending moments

6 Conclusions

In this study, a method for calculation of foundation pit retaining piles based on nonlinear Pasternak two-parameter foundation model is developed by combining the advantages of the Pasternak two-parameter foundation model and the nonlinear soil resistance–pile lateral displacement (*p*–*y*) curve and considering the nonlinearity of the soil stiffness on both sides of the retaining pile and the continuity of the lateral soil deformation. The following conclusions can be drawn:

(1) The pile displacements obtained from this study are analyzed by comparing them with the measured values and the results calculated by the *p*–*y* curve method based on the Winkler foundation model. It is found that when the conventional Winkler foundation model is used to calculate the foundation pit retaining pile, the pile horizontal displacement and internal force will be overestimated. It indicates that the shearing effect of the soil on the pile side contributes to the reduction of the pile horizontal displacement in a certain degree. The horizontal displacement obtained from this study is closer to the measured values, which verifies the rationality and applicability of the method proposed in this study.

(2) The Pasternak two-parameter foundation model makes up for the inherent defects of the Winkler single-parameter foundation model and considers the continuity of soil deformation. Therefore, it can better simulate the actual situation of pile–soil interaction, and has certain practical engineering significance.

(3) Combining the soil stiffness on both sides of the

retaining pile with the nonlinear *p*−*y* curve, it is found that the soil stiffness on the pile side is a nonlinear function of the pile lateral displacement.

(4) Using the transfer matrix method to solve the differential equation for the pile deflection can not only obtain the semi-analytical solution of the internal force and deformation of any pile section under the premise of ensuring the calculation accuracy, but also consider the pile−anchor deformation coordination problem through the point matrix.

References

[1] ZHU Jun-chen. Foundation pit monitoring and stability analysis of pump house in Sanmen Nuclear Power Phase II Project[J]. Chinese Journal of Underground Space and Engineering, 2019, 15(Suppl.1): 385−390.

[2] WU Yi-qian, ZHU Yan-peng. Monitoring and numerical simulation of deformation law of deep foundation pit of subway station in Lanzhou collapsible loess[J]. Chinese Journal of Geotechnical Engineering, 2014, 36(Suppl.2): 404−411.

[3] GUO Peng-xin, XIAO Yan, KUNNATH S K. Review of analysis methods for laterally loaded pile subjected to large displacement[J]. Journal of Natural Disasters, 2015, 24(3): 132−142.

[4] CHEN Bao-guo, YAN Teng-fei, WANG Cheng-peng, et al. Experimental study on compatible deformation of diaphragm wall support system for deep foundation pit[J]. Rock and Soil Mechanics, 2020, 41(10): 3289−3299.

[5] MA Jian-jun, WANG Man, LIU Jia-yu, et al. Model tests of nonlinear dynamic responses for laterally loaded long piles based on Winkler foundation theory[J]. Journal of Vibration and Shock, 2021, 40(1): 39−44, 67.

[6] ZHAO Ming-hua, LIU Tao, YANG Chao-wei, et al. Analysis on mechanical characteristics of laterally loaded piles by Newmark method considering steep slope effect[J]. Journal of Highway and Transportation Research and Development, 2014, 31(10): 58−64.

[7] ZHANG Wang-xi, YI Wei-jian, CHEN You-kun, et al. Analytical solutions about horizontal displacement of laterally loaded long-piles under double-parameter foundation[J]. Journal of Architectural Science and Civil Engineering, 2007(4): 34−38.

[8] LIANG Fa-yun, LI Yan-chu, HUANG Mao-song. Simplified method for laterally loaded piles based on Pasternak double-parameter spring model for foundations[J]. Chinese Journal of Geotechnical Engineering, 2013, 35(Suppl.1): 300−304.

[9] ZHU Yan-peng, WEI Sheng-hua. Research on interaction between deep excavation supporting pile and soil[J]. Rock and Soil Mechanics, 2010, 31(9): 2840−2844.

[10] ZHU Bi-tang, YANG Min. Comparison between elastoplastic method and *m*-method for retaining structures[J]. Chinese Journal of Geotechnical Engineering, 2006, 28(Suppl.1): 1387−1394.

[11] PASTERNAK P L. Fundamentals of a new method of analyzing structures on an elastic foundation by means of two foundation constants[M]. Moscow City: [s. n.], 1954.

[12] XU Ri-qing, CHENG Kang, YING Hong-wei, et al. Deformation response of a tunnel under foundation pit unloading considering buried depth and shearing effect[J]. Rock and Soil Mechanics, 2020, 41(Suppl.1): 195−207.

[13] TANAHASHI H. Formulas for an infinitely long Bernoulli-Euler beam on the Pasternak model[J]. Journal of the Japanese Geotechnical Society, 2004, 44(5): 109−118.

[14] YAO W J, YIN W X. Numerical simulation and study for super-long pile group under axis and lateral loads[J]. International Journal of Advanced Structural Engineering, 2010, 13(6): 1139−1151.

[15] ZHANG Hong. Research on analysis method of single pile under lateral load[D]. Harbin: Harbin Institute of Technology, 2012.

[16] WANG Guo-cui, YANG Min. Calculation of laterally loaded piles in clay[J]. Journal of Tongji University (Natural Science), 2012, 40(3): 373−378.

[17] CAO Wei-ping, XIA Bing, GE Xin. Formation and application of hyperbolic *p*-*y* curves for horizontally loaded single batter piles[J]. Journal of Zhejiang University (Engineering Science), 2019, 53(10): 1946−1954.

[18] WANG Teng, WANG Tian-lin. Experimental research on silt *p*−*y* curves[J]. Rock and Soil Mechanics, 2009, 30(5): 1343−1346.

[19] KIM T B, KIM N K, LEE W J, et al. Experimental load-transfer curves of laterally loaded piles in Nak-Dong river sand[J]. Journal of Geotechnical and Geoenvironmental Engineering, 2004, 130(4): 416−425.

[20] ZHU Y P, ZHOU Y. Analysis and design of frame supporting structure with prestressed anchor bars on loess slope[C]// ACMSM2004. Perth: [s. n.], 2004.

[21] VESIC A S. Bending of beams resting on isotropic elastic solids[J]. Journal of Soil Mechanics and Foundation Engineering, ASCE, 1961, 87(2): 35−53.

[22] RAJASHREE S S, SITHARAM T G. Nonlinear finite-element modeling of batter piles under lateral load[J]. Journal of Geotechnical and Geoenvironmental Engineering, 2001, 127(7): 604−612.

[23] ZHU Bi-tang. The ultimate resistance of soil and the behavior of laterally loaded piles[D]. Shanghai: Tongji University, 2005.

[24] China Academy of Building Research. JGJ120—2012 Technical specification for retaining and protection building foundation excavations[S]. Beijing: China Architecture & Building Press, 2012.

[25] LIU Qing-tan, NI Guo-rong. Transfer matrix method in structural analysis[M]. Beijing: China Railway Press, 1997.

[26] SUN Xun-fang, FANG Xiao-shu, GUAN Lai-tai. Mechanics of materials[M]. Beijing: Higher Education Press, 1994.

[27] FILHO R M, MENDONCA A V, PAIVA J B. Static boundary element analysis of piles submitted to horizontal and vertical loads[J]. Engineering Analysis with Boundary Elements, 2005, 29(3): 195−203.

[28] ZHOU Yong, SONG Xuan-bing. Displacement analysis of pile-anchor retaining structure based on *p*−*y* curve of horizontally loaded pile[J]. Building Science, 2019, 35(7): 46−52.

[29] Shandong Provincial Department of Architecture. GB50497—2009 Technical code for monitoring of building excavation engineering[S]. Beijing: China Planning Press, 2012.